

MASTER

SLAC-CN--331

DE86 012136

# SINGLE PASS COLLIDER MEMO CN-331

**TITLE:** PLIC SIGNAL VOLTAGES IN THE SLAC ACCELERATOR SCALED TO THE SLC ARCS

**AUTHORS:** T. M. Jenkins, W. R. Nelson and D. D. Reagan

**DATE:** 16 June 1986

**ABSTRACT.** To detect conditions and to forestall events in which an electron or positron beam might otherwise melt a hole in its SLC arc vacuum chamber, and to provide information on the magnitude and location of these and other, less harmful, beam losses, it is planned to install two PLIC\* cables along each arc, one on each side of the magnet string. A similar system (but with one long ion chamber) has been in use at SLAC for 20 years.

Electromagnetic shower calculations have been made to estimate the ion chamber signals which will be produced in the new system, making use of data from the old system.

It is estimated that a potentially damaging beam loss in a SLC arc will give rise to an ion chamber signal pulse with an amplitude in the order of 2 to 5 volts. Depending upon the location of a beam loss, sensitivity may vary from its average value by as much as 40 percent. Most of this signal is due to charged particles in the electromagnetic shower that are able to escape the magnetic field and reach PLIC.

## INTRODUCTION.

The PLIC along the SLAC accelerator provides a means of shutting off the machine in case of excessive local beam loss and furnishes diagnostic aid for operation of the beam. A similar PLIC system will be installed along the collider arcs. The purpose of this note is to better understand the nature of the signal that is to be expected from an inadvertant beam loss along these arcs using data taken with the accelerator PLIC system.

Measurements have been made by purposely steering a 7 GeV electron beam into a section of the SLAC accelerator wave guide<sup>3</sup>. A PLIC signal of  $V_0 = 2$  volts was observed, corresponding to an incident (scaled) beam power of  $P_0 = 10$  kW ( $H_0 = 360$  pps and  $T_0 = 1.6$   $\mu$ sec). Corresponding to the beam shutoff requirements of the SLC arcs, a power level of  $P = 720$  W (at  $H = 180$  pps) has been assumed for the present study. The pulse width of the SLC PLIC signal will be governed by the coaxial cable "bandwidth", and is expected to be  $T \approx 0.25$   $\mu$ sec.

## SIMPLE SCALING MODEL.

Under the assumption that the radiation environment for the two situations is the same (i.e., same spectrum and relative abundance), the voltage *expected* from the SLC PLIC can be obtained from that *measured* by the accelerator PLIC using

\* Panofsky Long Ion Chamber<sup>1,2</sup>.

EWD

the expression

$$\frac{V}{V_0} = \left( \frac{P}{P_0} \right) \left( \frac{T_0}{T} \right) \left( \frac{H_0}{H} \right) \left[ \frac{FS/2\pi R}{F_0 S_0/2\pi R_0} \right] \left( \frac{\bar{l}}{\bar{l}_0} \right) , \quad (1)$$

where SLAC accelerator quantities have zero subscript, and where

$F, F_0$  = fraction of energy escaping device (integrated along beam direction),

$R, R_0$  = distance from shower core to PLIC = 16 or 200 cm, respectively,

$S, S_0$  = arc length of circle subtended by PLIC  $\approx 2r$  or  $2r_0$ , respectively,

$r, r_0$  = outer radius of the PLIC cables = 3/16 or 3/4 in., respectively,

$\bar{l}, \bar{l}_0$  = mean chord length of particles traversing PLIC.

The mean chord length for randomly oriented particle trajectories through convex shaped volumes can be shown to be given by<sup>4</sup>

$$\bar{l} = \frac{4 \times \text{volume}}{\text{surface area}}.$$

For a cylinder of length  $L$  we obtain

$$\begin{aligned} \bar{l} &= \frac{(4)(\pi r^2 L)}{2\pi r L(1+r/L)} \\ &= \frac{2r}{1+r/L} \\ &\approx 2r \quad \text{for } r \ll L. \end{aligned}$$

After substituting the numerical values, we get

$$V = CV_0 \left( \frac{F}{F_0} \right) = 1.44 \left( \frac{F}{F_0} \right) , \quad (2)$$

where

$$C = \left( \frac{P}{P_0} \right) \left( \frac{T_0}{T} \right) \left( \frac{H_0}{H} \right) \left( \frac{r}{r_0} \right)^2 = 0.72 .$$

The fraction of energy leaking out of either device (i.e., SLC beam pipe or accelerator wave guide), as well as the similarities and differences of the two radiation environments, will be discussed in the following sections.

**SHOWER LEAKAGE CALCULATIONS.**

Using the EGS4 program<sup>5</sup>, shower calculations were done for the two situations in question: the SLAC accelerator wave guide and the SLC beam pipe (excluding the magnetic field, but with magnet iron in place). The fraction of shower energy exiting either device and reaching PLIC was determined for a variety of conditions (e.g., origin of shower, angle of incidence, etc.). Energy spectrum data was also obtained for both photons and charged particles. A full cylindrical geometry mockup was used for the accelerator wave guide calculations. However, for efficiency reasons, a semi-infinite slab geometry was used for the SLC arc calculations.

**SLC Arc Calculations**—The geometry shown in Figure 1 was used in the EGS4 simulation of the SLC arcs:\*

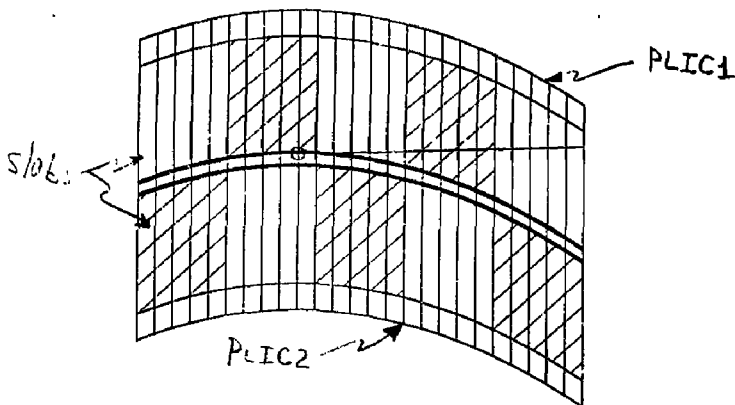


Fig. 1. EGS4 geometry used in SLC arc calculations.

In this figure the beam pipe is represented by the dark curved lines (actually, a pair of two closely spaced lines) that extend from left to right (along the general direction of the beam). The figure is purposely distorted such that the total horizontal distance represents 1250 cm, whereas the vertical distance covers about 16 cm on either side of the beam pipe. The cross-hatched areas represent magnet iron and the beam pipe material is aluminum. The rest of the regions in this geometry, including the center of the beam pipe, are vacuum. As we have indicated, this slab geometry is semi-infinite—i.e., the slabs extend forever into and out of the plane of the paper.

The curvature of the SLC arcs was approximated by rotating the “horizontal” sides of each slab by a slight amount while keeping the vertical sides of all slabs

---

\* User Code fileid=UCPLIC21 MORTTRAN

parallel to one another. The amount of curvature applied at each point of rotation was chosen such that the beam moved a distance of 1 cm after having traveled a distance of 250 cm (i.e., the distance associated with each of the five magnets depicted by the cross-hatching). It should be pointed out, however, that the overall results were not greatly affected by the addition of curvature to the geometry.

In Figure 1 the circle and ray indicate the location and direction, respectively, of an incident beam impinging upon the SLC beam pipe at a 1 mradian angle relative to the surface of the particular slab at that position. The curved lines at the very top and bottom of the figure designate the locations of the two PLIC cables, PLIC1 and PLIC2, respectively, that will be positioned 16 cm from the beam centerline.

Typical results are shown in Figure 2 (26 incident electrons at 50 GeV), where the energy reaching PLIC1 and PLIC2 is plotted as a function of the distance,  $X(cm)$ , along the beam direction. A significant fraction of the total incident beam energy is observed to reach the PLIC surfaces—9.8% at PLIC1 and 3.7% at PLIC2, of which 40-60% is in the form of photon radiation (i.e., 3.7% and 2.3% for PLIC1 and PLIC2, respectively, in Figure 2). The average energy of the photon radiation reaching either PLIC is 1 to 2 MeV, whereas the average charged particle energy is 10 to 20 MeV. The fraction of energy deposited in various slabs of the magnet iron is also shown as a matter of general interest.

In order to determine if there is a situation in which the shower leakage is effectively "hidden" from either or both PLICs, a series of calculations was done for incident beam positions varying from 50 cm to 550 cm. The results are shown in Figure 3 for a beam directed toward PLIC1, and in Figure 4 for a beam directed toward PLIC2. Solid lines have been drawn through the points for the two PLICs and a dotted line through the *sum* of the two signals, which is the quantity of interest in Eq. (2). The energy percentage seen by an individual PLIC ranges from 2 to 20%. The sum, however, only varies from 12 to 22% because when one PLIC becomes "hidden" the other becomes "visible", and values in this range will be used in Eq. (2).

The results of all the EGS4 calculations for the SLC arcs are summarized in Table 1.

#### DISCLAIMER

This report was prepared as an account of work sponsored by an agency of the United States Government. Neither the United States Government nor any agency thereof, nor any of their employees, makes any warranty, express or implied, or assumes any legal liability or responsibility for the accuracy, completeness, or usefulness of any information, apparatus, product, or process disclosed, or represents that its use would not infringe privately owned rights. Reference herein to any specific commercial product, process, or service by trade name, trademark, manufacturer, or otherwise does not necessarily constitute or imply its endorsement, recommendation, or favoring by the United States Government or any agency thereof. The views and opinions of authors expressed herein do not necessarily state or reflect those of the United States Government or any agency thereof.

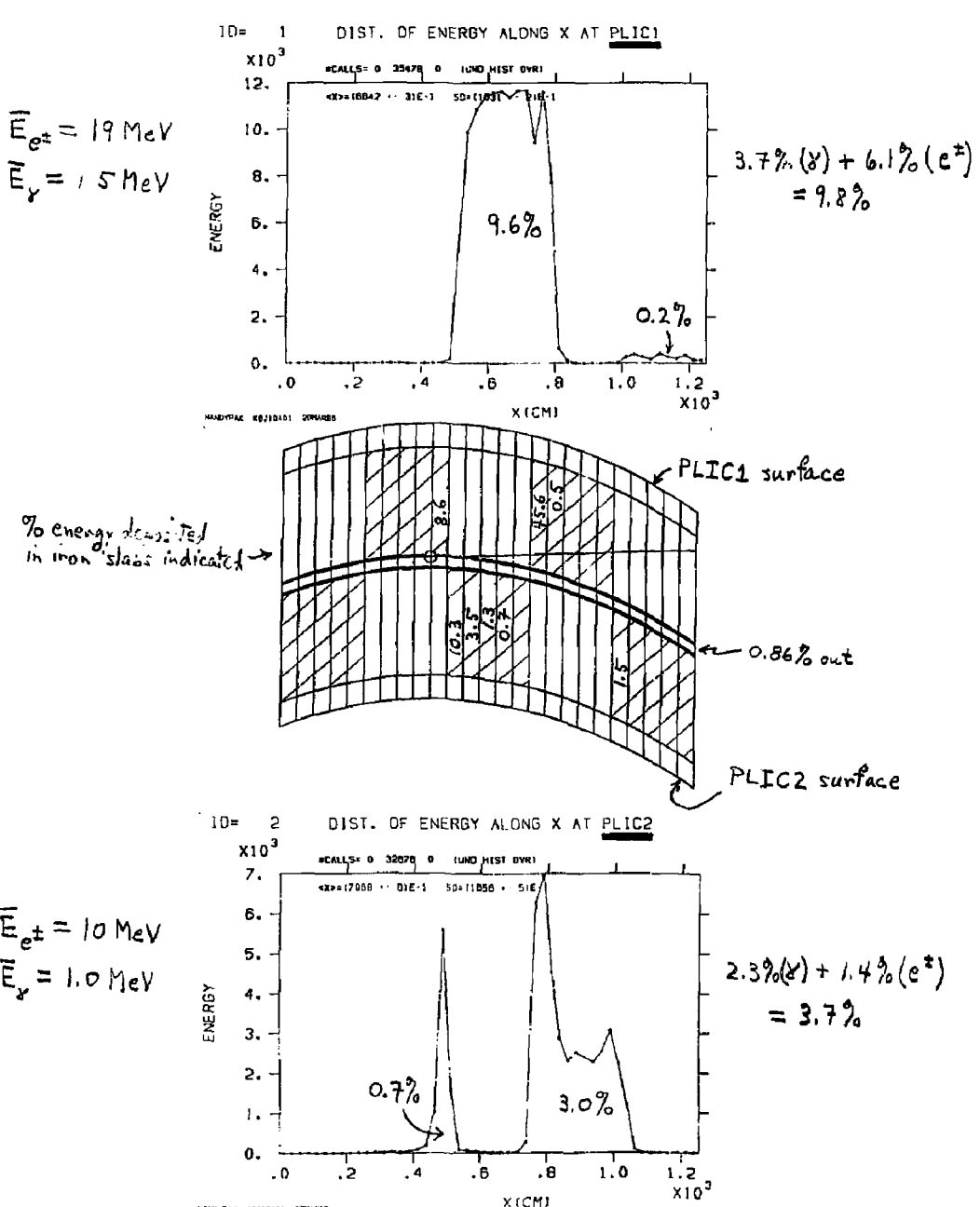


Fig. 2. Energy reaching surfaces of PLIC1 and PLIC2.

Table 1. Summary of EGS4 calculations for SLC PLICs.

Run ID	Beam Location (cm)	Beam Direction	Radiation Component	PLIC1	PLIC2	PLIC1 + PLIC2
K6J2A01	50	Toward PLIC1	$\gamma$	2.07	3.86	5.93
			$e^\pm$	6.06	1.95	8.01
			$\gamma + e^\pm$	8.13	5.81	13.94
K6J4A01	150	Toward PLIC1	$\gamma$	1.32	6.22	7.54
			$e^\pm$	2.22	6.18	8.40
			$\gamma + e^\pm$	3.54	12.40	15.94
K6J6A01	250	Toward PLIC1	$\gamma$	0.87	6.75	7.62
			$e^\pm$	1.13	12.55	14.68
			$\gamma + e^\pm$	2.00	20.30	22.30
K6J8A01	350	Toward PLIC1	$\gamma$	1.80	4.38	6.18
			$e^\pm$	2.37	8.16	10.53
			$\gamma + e^\pm$	4.17	12.54	16.71
K6J10A01	450	Toward PLIC1	$\gamma$	3.69	2.29	5.98
			$e^\pm$	6.09	1.43	7.52
			$\gamma + e^\pm$	9.78	3.72	13.50
K6J12A01	550	Toward PLIC1	$\gamma$	2.07	3.53	5.60
			$e^\pm$	6.08	1.65	7.73
			$\gamma + e^\pm$	8.15	5.18	13.33
K4J2A01	50	Toward PLIC2	$\gamma$	2.32	5.33	7.65
			$e^\pm$	4.79	8.19	12.98
			$\gamma + e^\pm$	7.11	13.52	20.63
K4J4A01	150	Toward PLIC2	$\gamma$	1.71	4.16	5.87
			$e^\pm$	2.53	6.57	9.10
			$\gamma + e^\pm$	4.24	10.73	14.97
K4J6A01	250	Toward PLIC2	$\gamma$	2.08	3.23	5.31
			$e^\pm$	2.24	7.22	9.46
			$\gamma + e^\pm$	4.32	10.45	14.77
K4J8A01	350	Toward PLIC2	$\gamma$	2.01	3.58	5.59
			$e^\pm$	2.90	2.55	5.45
			$\gamma + e^\pm$	4.91	6.13	11.04
K4J10A01	450	Toward PLIC2	$\gamma$	2.84	5.79	8.63
			$e^\pm$	5.74	5.87	11.61
			$\gamma + e^\pm$	8.58	11.66	20.24
K4J12A01	550	Toward PLIC2	$\gamma$	2.14	5.54	7.78
			$e^\pm$	4.75	8.44	13.19
			$\gamma + e^\pm$	6.89	13.98	20.87

Note: The numbers above give the percentage of the total incident energy reaching one or both PLICs.

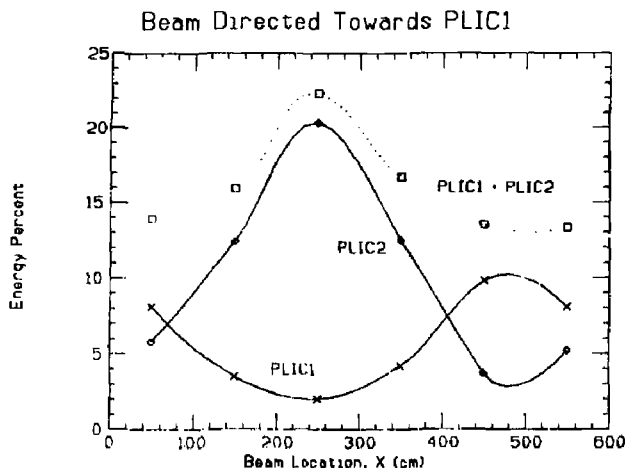


Fig. 3. PLIC signals vs. incident beam location.

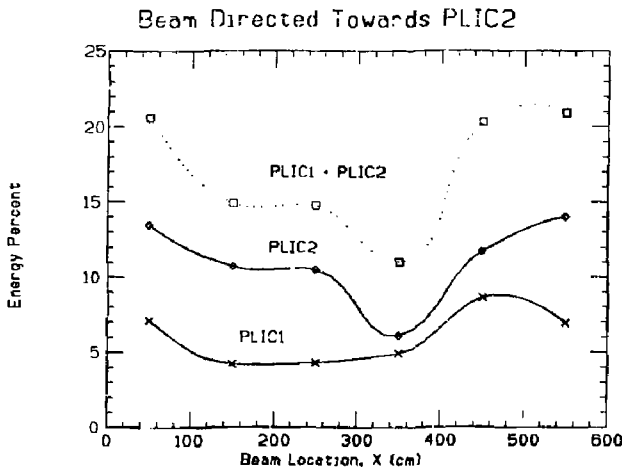


Fig. 4. PLIC signals vs. incident beam location.

Accelerator Wave Guide Calculations—EGS4 calculations were also performed in order to simulate the radiation escaping from a wave guide and reaching the PLIC in the SLAC accelerator tunnel\*. A full cylindrical geometry mockup of the wave guide was made using dimensions taken from reference 2 (which are consistent with those in the SLAC Big Book<sup>6</sup> ). An accelerator length of 30 meters was used and

\* User Code fileid=UCTPLIC1 MORTTRAN.

the radiation emanating from the device was scored at a radial distance of 200 cm, corresponding to the actual location of the PLIC in the SLAC tunnel\*.

The distribution of the energy reaching PLIC along its length is shown in Figure 5, where essentially all of the signal is induced within a distance of about 15 meters measured from the shower origin. This is consistent with experimental observation<sup>3</sup>.

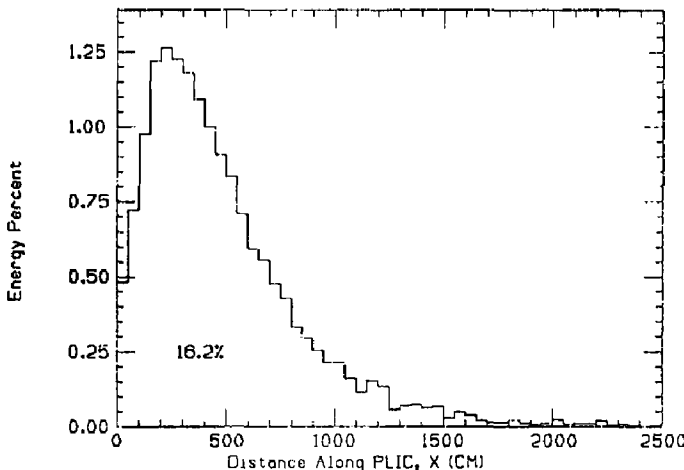


Fig. 5. Energy reaching the SLAC accelerator PLIC.

The total percentage within the histogram is 16.2%. Using this value of  $F_D$  in Eq. (2), together with  $12\% \leq F \leq 22\%$ , we obtain SLC PLIC voltages ranging from 1 to 2 volts. This result is valid provided that the radiation environments of the two situations are identical (or reasonably so). We will now show that this is not really the case and that a better scaling model is required.

The energy distribution of the photons and the charged particles was also scored for the SLAC tunnel case and the average energy was found to be about 1 MeV for photons and 10 MeV for charged particles—i.e., the quality of the radiation spectra is essentially the same as for the SLC arc situation.

However, contrary to the SLC arc example in Figure 2 in which 40-60% of the energy reaching the PLICs is in the form of photons, almost all of the energy reaching the accelerator PLIC is accounted for by photons (i.e.,  $15.0\%(\gamma) + 1.2\%(e^\pm) = 16.2\%$ ). An interesting and important question is therefore raised concerning whether the signal measured by the PLIC in the SLAC tunnel is caused by charged particles or photons escaping from the accelerator section, since the latter must first convert into charged particles in order to register a signal in the PLIC

---

\* Vacuum was used instead of air with no appreciable change in the results.

gas. Furthermore, since the range of a 10 MeV electron is 4.3 meters in air and 0.6 cm in copper, a large number of the shower electrons will enter the PLIC gas, particularly in the SLC arc case since the path through the air is smaller and the electron-photon ratio is so much larger (e.g., see Table 1).

To answer the question regarding which component causes the signal, the cylindrical geometry used by EGS4 in the tunnel simulation was modified\* to include three cylindrical shells starting at the PLIC distance,  $R_0 = 200$  cm, representing:

1. the PLIC cable insulation (1/8 inch polyethylene),
2. the outer wall of the cable (1/16 inch copper), and
3. the gas region (13/16 inch of argon at 2 atm.).

A precise geometry mockup is not expected to be important, although the thickness of each layer should match reasonably well those of the accelerator PLIC. Charged particles were tagged as they left the wave guide and passed through the 200 cm vacuum toward the insulation-copper-gas. The energy deposition in the gas was then scored by component. The results are given in Table 2 below.

Table 2. Energy conversion summary (accelerator PLIC simulation).

Radiation Component	Wave Guide Leakage	Deposition in Insulation-Wall	Deposition in Argon Gas	Discard Region	Conversion Efficiency
$\gamma$	15.0%	1.60%	3.81%	9.60%	$\alpha_\gamma = 3.81/15.0 = 0.254$
$e^\pm$	1.20%	0.470%	0.390%	0.340%	$\alpha_e = 0.390/1.20 = 0.325$
$\gamma + e^\pm$	16.2%	2.10%	4.20%	9.90%	$\alpha_\gamma + \alpha_e = 0.579$

From this table one can calculate the *relative conversion efficiency*,  $\alpha$ , for photons in a PLIC-like device; namely,

$$\alpha = \frac{\alpha_\gamma}{\alpha_\gamma + \alpha_e} = 0.44 , \quad (3)$$

which will be used in an improved scaling model that will be presented next.

---

\* User Code fileid= UCTPLIC2 MORTTRAN.

**AN IMPROVED SCALING MODEL.** We will assume that the relative conversion efficiency of photons, as determined in the previous section for the accelerator PLIC, can be applied to the case of the PLICs in the SLC arcs. Generalizing Eq. (2) into component form gives

$$V_\gamma = CV_{0\gamma} \left( \frac{F_\gamma}{F_{0\gamma}} \right)$$

and

$$V_e = CV_{0e} \left( \frac{F_e}{F_{0e}} \right) ,$$

where  $V = V_\gamma + V_e$  is the voltage *expected* from the SLC PLIC system (i.e., PLIC1 + PLIC2 total). The voltage *measured* with the accelerator PLIC can be written

$$V_0 = V_{0\gamma} + V_{0e} = \alpha V_0 + (1 - \alpha) V_0 ,$$

where  $\alpha$  is given by Eq. (3). Combining these expressions, we get

$$V = CV_0 \left[ \alpha \frac{F_\gamma}{F_{0\gamma}} + (1 - \alpha) \frac{F_e}{F_{0e}} \right] , \quad (4)$$

where in the previous section we obtained

$$F_{0\gamma} = 15.0\% ,$$

$$F_{0e} = 1.20\% ,$$

$$\alpha = 0.44 ,$$

and where the values for  $F_\gamma$  and  $F_e$  are given in Table 1.

For example, the PLIC signal corresponding to the SLC arc case shown in Figure 2 (i.e., Run ID K6J10A01 of Table 1) gives:

$$V = (0.72)(2.0) \left[ 0.44 \left( \frac{5.98}{15.0} \right) + (1 - 0.44) \left( \frac{7.52}{1.20} \right) \right] = 5.3 \text{ volts} .$$

Using the data from Table 1 with Eq. (4), the PLIC signal voltages (PLIC1 + PLIC2) are plotted in Figure 6 as a function of the location of the incident beam along the magnet structure for the two beam directions (toward PLIC1 or toward PLIC2).

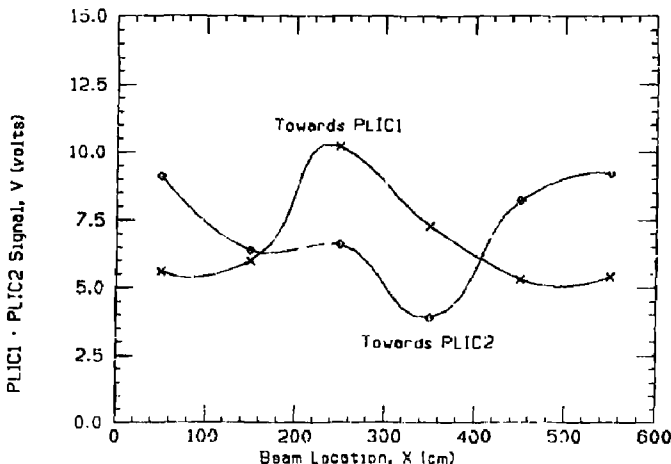


Fig. 6. PLIC1 + PLIC2 signal vs. incident beam location.

The voltages, which range from 3 to 10 volts, are higher than the 1-2 volt numbers calculated previously with the simpler model. However, the magnetic field associated with the SLC arc was not taken into account in any of the calculations presented in this study. Under the extreme condition where none of the charged particles reach PLIC (i.e.,  $F_e = 0$ ), Eq. (4) tells us that the PLIC signal voltage would only be 0.25 to 0.36 volts.

**CONCLUDING REMARKS.** The calculations indicate that the leakage of charged particles from the relatively thin SLC beam pipe will give PLIC signals in the range of 0.3 to 10 volts, depending on the conditions under which the incident beam is lost along the arcs and the effect of the magnetic field. Extending these numerical calculations to include the transport of charged particles in a magnetic field would prove difficult and expensive, and therefore has not been done.

A relativistic electron with energy,  $W$ , emitted perpendicular to the pipe in a horizontal plane will have sufficient momentum to cross a fringing magnetic field,  $B(x)$ , if  $W > ce \int B(x) dx$ , which for a SLC arc magnet is about 6 MeV. For particles emitted parallel to the beam pipe the energy only has to be 3 MeV. Crudely speaking, particles of one polarity will be deflected back into the pipe; their opposites may cross the field to the ion chamber. A reasonable guess may be that all the photon and half the charged particle energy indicated in Table 1 contributes to the signal. Applying this guess with Eq. (4) gives PLIC signals in the range of 2 to 5 volts.

## REFERENCES

1. W. K. H. Panofsky, "The Use of a Long Co-axial Ion Chamber Along the Accelerator", SLAC TN-63-57 (1963).
2. H. DeStaebler, "Note on Panofsky's Long Ion Chamber", SLAC TN-63-63 (1963).
3. M. Fishman and D. Reagan, IEEE Trans. Nuc. Sci. NS-14, No. 3 (1967) 1096.
4. M. G. Kendall and P. A. P. Moran, *Geometrical Probability* (Hafner Publishing Co., New York, 1963).
5. W. R. Nelson, H. Hirayama, and D. W. O. Rogers, "The EGS4 Code System", SLAC-265 (1985).
6. R. B. Neal (General Editor). *The SLAC Two-Mile Accelerator* (W. A. Benjamin, Inc., 1968).